



EXPERIMENTAL STUDY ON THE SEISMIC PERFORMANCE OF EXTERNALLY CONFINED REINFORCED CONCRETE COLUMNS

Munawar A. HUSSAIN¹ and Robert G. DRIVER²

SUMMARY

Due to changes in codes, poor detailing practice, rezoning of seismic activity, and/or a change of function of the buildings requiring changes in performance objectives, many existing reinforced concrete buildings are seismically deficient. A scheme for the rehabilitation of seismically deficient reinforced concrete buildings is proposed that makes use of unstiffened thin steel plate shear walls, which are becoming increasingly popular as a lateral load resisting system in the construction industry. The connection of the unstiffened steel plate shear walls to the columns of the reinforced concrete frame is made with collars fabricated from steel hollow structural sections (HSS) and the connection to the beams of the frame is made either with collars or bolts passing through the slab. The steel collars serve not only as a means of connection to the steel plate, but they also increase the strength, ductility, and robustness of the concrete frame members. The objective of the present research is to investigate the performance of the proposed seismic rehabilitation scheme which is, in fact, a composite lateral load resisting system consisting of steel plate shear walls and a reinforced concrete frame. This paper presents a summary of the first two phases of the project: behaviour of the externally confined columns under concentric monotonic loading (phase I) and under simulated seismic loading (phase II).

INTRODUCTION

Various rehabilitation schemes have been developed for the upgrade of seismically deficient reinforced concrete buildings. A large number of reinforced concrete buildings have been seismically upgraded and there are still many more to be rehabilitated. The collapse or damage of seismically deficient reinforced concrete buildings in the most recent earthquakes have confirmed the existence of a large number of seismically deficient reinforced concrete buildings which are a potential threat to the lives of thousands of people around the globe.

Figure 1(a) shows a schematic diagram of the proposed rehabilitation scheme, which consists of unstiffened steel plate shear walls installed in a deficient reinforced concrete building. These walls resist the lateral loads through the development of a diagonal tension field after out-of-plane buckling of the steel plates occurs at relatively low loads. Large-scale testing has confirmed that these walls provide an excellent lateral load resisting system both for wind and earthquake loading [1]. These walls have high

¹ Doctoral Candidate, Department of Civil and Environmental Engineering, University of Alberta.

² Associate Professor, Department of Civil and Environmental Engineering, University of Alberta.

initial stiffness, low weight, redundancy, high deformability (ductility), and high hysteresis damping (energy dissipation capability). There is no evidence in the literature about the use of this type of steel plate shear wall for the seismic rehabilitation of reinforced concrete buildings. However, a few reinforced concrete buildings have been seismically upgraded in North America with the help of stiffened steel plate shear walls. The seismic performance of unstiffened steel plate shear walls as a lateral load resisting system, has already been validated by Driver *et al.* [1]. Therefore, the present research focuses on the performance of the seismically deficient reinforced concrete frame members confined externally by HSS collars. The function of the collars is two-fold: (a) provide a means of connection between the steel plate shear wall panels and the reinforced concrete frame; and (b) improve the ductility and energy dissipation at the location of plastic hinges through confinement. Figure 1 also shows representative HSS collars with bolted as well as welded corner connections and a conventional rebar hoop that meets seismic detailing requirements for comparison. In contrast to the conventional hoop reinforcement in which confining pressure is principally contributed by the axial stiffness of the hoop bars, the confining pressure under the collars is contributed significantly by both axial as well as flexural stiffness of the sides of the collars, as demonstrated by Hussain and Driver [2] through finite element study.

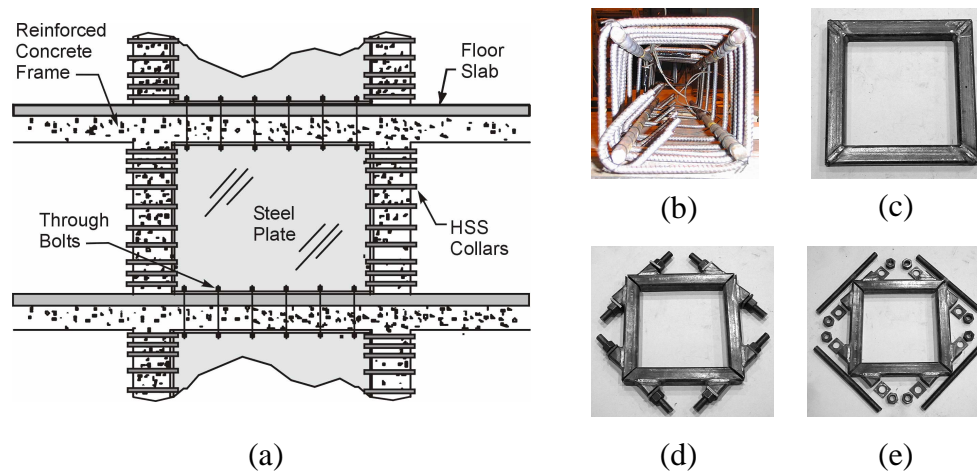


Figure 1: (a) Schematic diagram of the proposed rehabilitation system; (b) conventional rebar hoop reinforcement; (c) HSS collar with welded collar connection; (d) HSS collar with bolted collar connection (assembled view); and (e) HSS collar with bolted collar connection (exploded view).

EXPERIMENTAL PROGRAMME

The experimental programme consists of two phases: (1) investigation into the behaviour of externally confined columns under monotonic concentric loading; and (2) investigation into the behaviour of externally confined columns under simulated seismic loading, with and without axial load.

Description of Specimens

Table 1 gives the internal and external transverse reinforcement details for specimens of phase I and phase II. In phase I of the experimental program, a total of 11 columns of 300x300 mm cross-section and 1500 mm in height were cast and tested. Of the 11 test columns, two (C00A and C00B) were control columns with conventional tie reinforcement and the remainder (C01 through C09) had external collar confinement. Each column had four nominally 20 mm diameter longitudinal bars, making the longitudinal reinforcement ratio equal to 1.33%. The effective concrete cover to the centroid of the longitudinal bars was kept equal to 58 mm. In placing the

transverse reinforcement, the columns were divided into three parts: top end zone; test region; and bottom end zone. The top and bottom end zones were 350 mm in height and the test region was 800 mm long. Columns C01 through C09 had external confinement by HSS collars and, in order to study the effect of external confinement separately, no tie reinforcement was provided in the test region. Figure 2(a) and 2(b) show representative test specimens with bolted and welded collars in the setup. The tie reinforcement in the test region of column C00A satisfied the gravity load design criteria of ACI 318-02 and CSA Standard A23.3-94 and the tie reinforcement of column C00B satisfied the seismic plastic hinge requirements of these codes. In the end zones of all columns, closely spaced ties as well as closely spaced, flexurally stiff external collars were provided to prevent failure from occurring near the reaction points. In the test regions of the collared columns, either four, six, or eight collars at equal spacings were used. The collars on column C01 were tightened to be just snug with the column, minimizing the active confinement pressure, and the pretensioning force in the bolts is considered to be negligible. In the cases of columns C02, C03, C04, and C05, a significant initial pretensioning force was applied to the bolts, which was measured with an annular load cell. The initial tensions in the bolts for these columns were 65.1 kN, 145.9 kN, 68.9 kN, and 90.2 kN, respectively. The bolts for column C03 had a significantly higher preload in order to study the potential benefits of active confining pressure.

Table 1—Description of specimens and transverse reinforcement details

Phase	Specimen	Transverse Steel						
		Steel Type	Size (mm)	s (mm)	s' (mm)	Corner Connection Type	A_t (mm ²)	ρ_t
I	C00A	Rebars	$\phi 10$	267	257	135-deg hooks	100	0.70
	C00B		$\phi 15$	70	55	135-deg hooks	200	5.19
	C01	HSS Collars	HSS 51x51x6.35	122	71	bolted	375*	4.81
	C02		HSS 76x51x6.35	122	71	bolted	375*	5.15
	C03		HSS 76x51x6.35	122	71	bolted	375*	5.15
	C04		HSS 76x51x6.35	170	119	bolted	375*	3.68
	C05		HSS 76x51x6.35	95	44	bolted	375*	6.63
	C06		HSS 51x51x6.35	122	71	welded	1085	13.92
	C07		HSS 76x51x6.35	122	71	welded	1375	18.90
	C08		HSS 102x51x6.35	122	71	welded	1734	25.48
	C09		HSS 76x51x6.35	170	119	welded	1375	13.50
II	CL0		Rebars	$\phi 15$	70	55	135-deg hooks	200
	CL1	HSS Collars	HSS 76x51x6.35	101	50	welded	1318	21.80
	CL2		HSS 76x51x6.35	151	100	welded	1318	14.58
	CL3		HSS 76x51x6.35	101	50	welded	1318	21.80
	CL4		HSS 51x51x6.35	101	50	welded	998	15.42
	CL5		HSS 76x51x6.35	101	50	welded	1318	21.80
	CL6		HSS 76x51x6.35	151	100	welded	1318	14.58
	CL7		HSS 76x51x6.35	101	50	welded	1318	21.80
	CL8		HSS 51x51x6.35	101	50	welded	998	15.42

* based on cross-sectional area of the bolts

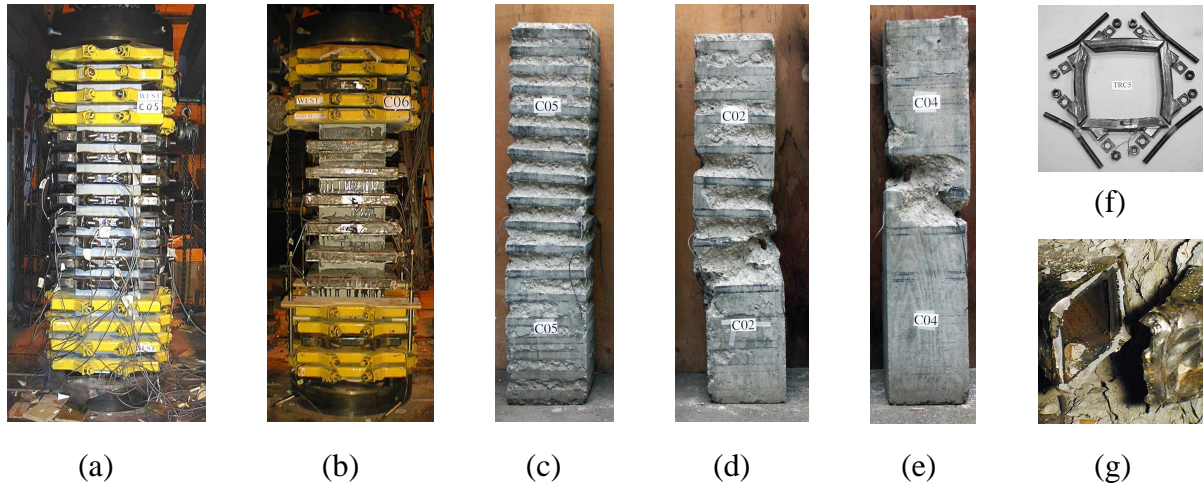


Figure 2: (a) Column C05 with bolted collars in the setup; (b) column C06 with welded collars in the setup; (c) column C05 at the end of the test after removing collars; (d) column C02 at the end of the test after removing collars; (e) column C04 at the end of the test after removing collars; (f) a typical deformed bolted collar at the end of the test; and (g) a typical fractured corner of a welded collar

In phase II of the experimental program, a total of nine full-scale column specimens (CL0 to CL8) were designed to simulate typical columns of two to three storey reinforced concrete buildings in seismic regions. All the columns were 300x300 mm in cross-section and reinforced with eight longitudinal steel bars of 25 mm diameter, constituting a longitudinal reinforcement ratio of 4.4%. Concrete cover of 60 mm was provided to the centroid of the vertical bars. Column CL0 was a control column and was provided with conventional tie reinforcement in the test region, which satisfied the seismic plastic hinge requirements of ACI 318-02 and CSA Standard A23.3-94. The spacing of the first hoop was set equal to $s/2$ above the footing in this column, where s is the typical centre-to-centre hoop spacing of 70 mm. All the remaining columns were provided with external transverse reinforcement by HSS collars in the test regions. In order to study the effect of external confinement separately, no internal tie reinforcement was provided in the test regions of these columns.

All the columns had 1800x1050x591 mm footings which were anchored to the strong floor of the structural laboratory by four post-tensioned 50 mm diameter high strength steel threaded rods to achieve fixity at the bases of the columns. The column reinforcement cages were erected vertically into the footings before casting the footing concrete. There was no splicing of the vertical bars in the columns. Casting of the columns and the footings was done separately. At the location of the construction joint between the columns and footings, the footing surface was roughened before the hardening of the concrete. Figure 3 shows the arrangement of the collars and the loading position of the columns with long and short shear spans. Columns CL0 to CL4 were tested with long shear spans and columns CL5 to CL8 were tested with short shear spans. On columns CL1 to CL4, heavy collars were provided in the region between the test region and the bracing channels to prevent failure at that location. Table 2 summarizes cylinder strength of concrete, axial load, axial load index (axial load/ $0.85 A_g f'_c$), and dimensions H1, H2, and H3 for all the columns used in this study. H1 represents the overall height of the concrete column measured from the top of the footing. H2 (height to horizontal load point) and H3 (height to vertical load point at the knife edge) have been defined in Figure 3. Specimens CL1 to CL8 were provided with external confinement by HSS collars in the test region, the height of which was kept approximately equal to 600 mm based on the premise that the plastic hinge length will not exceed the test region. The clear

spacing between the collars, s' , was either 50 or 100 mm. The clear distance between the top of the footing and the bottom of the first collar was equal to $s'/2$.

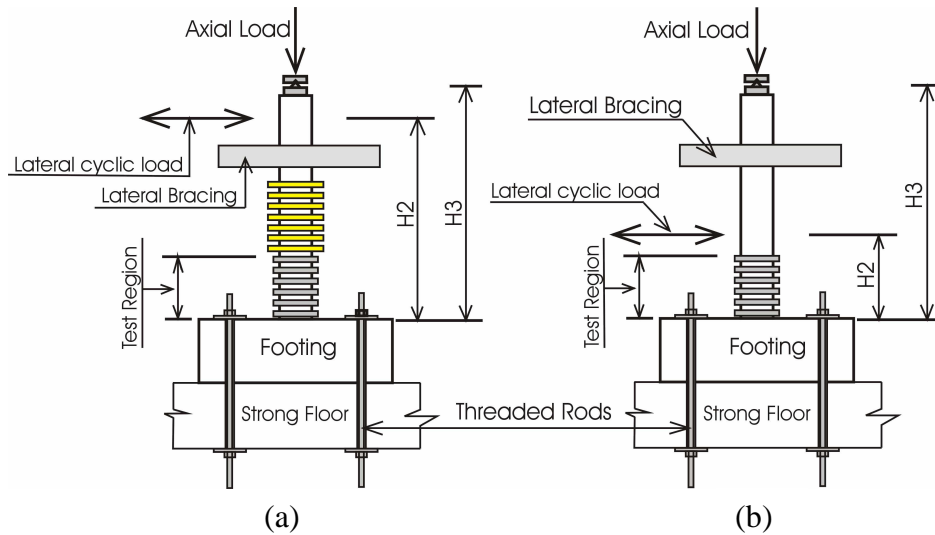


Figure 3: Loading scheme: (a) with long shear span; (b) with short shear span

Three sizes of HSS were used in the fabrication of the collars used in this study (dimensions in mm): HSS102x51x6.35, HSS76x51x6.35, and HSS51x51x6.35. The HSS collar segments were oriented so that the largest flexural stiffness was available to resist lateral expansion of the concrete in the column and were bevelled at 45° at the corner connections. In the case of collars with bolted corner connections, 25.4 mm diameter high strength threaded rods were used to make the connection between the HSS sides. The fabrication of collars for phase I was done in the structural engineering laboratory at the University of Alberta. A partial penetration single-V groove weld was deposited all around the attachments in case of the bolted collars and around the corner joints in the case of the welded collars, using the shielded metal arc welding process. The fabrication of the welded collars for phase II was done in a commercial fabrication workshop with full penetration groove welds all around the corners. Installation of the bolted collars, which requires the clamping of the bolted collars onto the column, is relatively easy. The installation of the welded collars was relatively more labour-intensive. The inner dimensions of the welded collars were kept 10 to 12 mm larger than those of the column cross-section. The welded collars are threaded on to the column, a method that obviously could not be used for rehabilitation in the field. The gap between the collar and the concrete column was filled with low viscosity epoxy grout; the performance of epoxy grout under shear and normal stresses in strengthened concrete structures has already been validated by Hussain *et al.* [3].

The volumetric ratios of transverse confining steel, ρ_t , for all of the test columns of phase I and phase II are given in Table 1. The volume of the confining steel for the welded collars was calculated by multiplying the cross-sectional area of the HSS by the perimeter of the collar measured at the centroid of the HSS cross-section. For the bolted collars, since the contribution of the HSS to confinement is limited by the behaviour of the bolts, the volume of the confining steel was taken as the net cross-sectional area of the bolts running at the centreline of the collars. In both cases, since the collars are placed externally and prevent most of the spalling, the volume of the concrete was calculated based on the gross area of the

column and the centre-to-centre vertical spacing of the collars. Hence, the core of the collared columns was considered equal to the cross-sectional dimensions of the columns. For columns C00A, C00B, and CL0, the volume of the tie steel was calculated in the same way as that for the collars, but the volume of the concrete was based on the core of the column within the reinforcing cage. The core dimension for C00A was 215x215 mm and for C00B and CL0 was 220x220 mm, based on the centreline of the ties.

Table 2—Concrete properties and location of loading points and plastic hinge lengths

Phase	Specimen	Cylinder Strength for Concrete				Axial Load kN	Axial Load Index	Location of Horizontal and Vertical Loads								
		Columns		Footings				H1 mm	H2 mm	H3 mm						
		f'_c MPa	σ MPa	f'_c MPa	σ MPa											
I	C00A	34.4	3.21	—	—	—	—	—	—							
	C00B	35.0	4.23													
	C01	37.9	1.20													
	C02	38.7	2.11													
	C03	37.8	1.90													
	C04	37.8	1.73													
	C05	36.4	1.05													
	C06	34.8	2.83													
	C07	47.0	1.41													
	C08	52.8	1.55													
C09	36.3	3.25	—	—	—	—	—	—								
II	CL0	32.7							0.51	31.1	1.52	1470/720	0.50/0.24	2075	1900	2200
	CL1	12.3							2.69	40.0	1.73	0	0	2075	1900	—
	CL2	15.9							1.01	32.2	0.56	720	0.50	2075	1900	2200
	CL3	15.4							1.36	33.1	1.31	720	0.52	2075	1900	2200
	CL4	32.7							0.77	38.6	1.46	720	0.24	2075	1900	2200
	CL5	26.3							1.19	46.2	2.34	0	0	2075	750	—
	CL6	32.6							1.54	43.3	1.18	720	0.25	2125	760	2250
	CL7	35.4							1.54	44.4	0.88	720	0.23	2125	755	2245
	CL8	35.3	1.41	45.9	0.85	720	0.23	2125	775	2250						

Material Properties

The average ultimate concrete strengths, f'_c , and the corresponding standard deviations for the specimens of phase I and phase II are given in Table 2. Poisson's ratio was determined using 100x200 mm cylinders and was found to have an overall mean value of 0.15. The mechanical properties of rebars, threaded rods, and HSS for both phases are given in Table 3. Strain-hardening strains and strain-hardening moduli are given only for steel with a well-defined yield plateau.

Loading Protocol

Phase I columns were tested under concentric monotonic axial loading. Initially, a load of about 200 kN was applied to each column to check the instrumentation and data acquisition system and then removed. Most columns were then loaded monotonically to failure, however one column with bolted collars (C05) and one with welded collars (C07) were subjected to 15 cycles of load from zero to near their respective

compressive capacities and back, in order to examine the robustness of the system. In particular, the cycles were to verify that the collars would not decrease in their effectiveness of confining the concrete in the columns due to deterioration or slip as the confining pressure was repeatedly applied and released. All the columns were tested under stroke control. The strain rate effect on the strength of the concrete of the columns tested in phase I is considered negligible.

Table 3—Properties of steel rebars and steel HSS

Phase	Steel Type	Size mm	f_y MPa	E_s MPa	f_p MPa	ϵ_p	ϵ_{sh}	H' MPa
I	Rebars	$\phi 10$	450	202 800	717	0.1000	—	—
		$\phi 15$	453	202 250	617	0.1350	0.0150	3863
		$\phi 20$	431	205 100	668	0.1150	0.0062	9837
	Threaded rods	$\phi 25$	811	202 100	950	0.0610	—	—
	HSS	HSS 51x51x6.35	497	203 400	642	0.0887	—	—
		HSS 76x51x6.35	445	202 700	506	0.0234	—	—
HSS 102x51x6.35		410	201 350	489	0.0166	—	—	
II	Rebars	$\phi 15$	517	206 800	802	0.1070	—	—
		$\phi 25$ (CL0 TO CL4)	510	199 930	710	0.0600	0.0110	8529
		$\phi 25$ (CL5 TO CL8)	515	199 795	687	0.1370	0.0170	5377
	HSS	HSS 51x51x6.35	464	202 140	601	0.1004	—	—
		HSS 76x51x6.35	512	206 660	660	0.0415	—	—

Phase II columns were tested under simulated seismic loading (constant axial load and lateral cyclic loading). After checking that all of the instrumentation was functioning properly, the vertical load was applied, followed by the horizontal cyclic loading. The cycles of horizontal loads were applied in the north-south direction. The columns were pushed initially in the north direction, after the application of gravity loads. For all of the columns, the vertical load was kept constant throughout the tests except for column CL0, in which a load of 1470 kN was applied from cycles 1 to 16 and 720 kN from cycle 17 to the end of the test. When the column reached large displacements, the P- Δ effect from the high vertical load caused a substantial drop in the applied lateral force in each displacement increment. For this reason, the vertical load was reduced to 720 kN and the test was continued. All the remaining columns were tested under 720 kN or zero load as per Table 1. The sequence for horizontal loading shown in Figure 4, which has been adapted from Ref. [4], was used for all the columns. The first five cycles were load controlled, in which a peak horizontal load of 75 percent of the lateral load V_y was applied. V_y is defined as the lateral force corresponding to the yield moment of the column, under axial load if present, taken as the point of first yield of the vertical tensile steel. The concrete stress distribution for the collared columns is based on the estimated confined material curves determined from the test results of phase I columns. A more general confined material model is currently under development and will eventually be used to define the confined concrete material curves for the phase II columns which, in turn, will be used to determine the yield displacements which may be slightly different from the values reported here. As shown in Figure 4(a), the yield displacement is defined using the first full cycle by extrapolating straight lines from the origin through the peak load-displacement points at $0.75V_y$ to the theoretical strength V_y .

The average of the yield displacements in the positive and negative directions was taken as the yield displacement (Table 3). The displacement ductility factor, μ_{Δ} , is defined as the ratio of the actual displacement to the yield displacement. Subsequent cycles were displacement controlled and extended to displacement ductilities, μ_{Δ} , equal to 1.5, 2, 4, 6, 8 and so on, with five cycles carried out at each displacement ductility level.

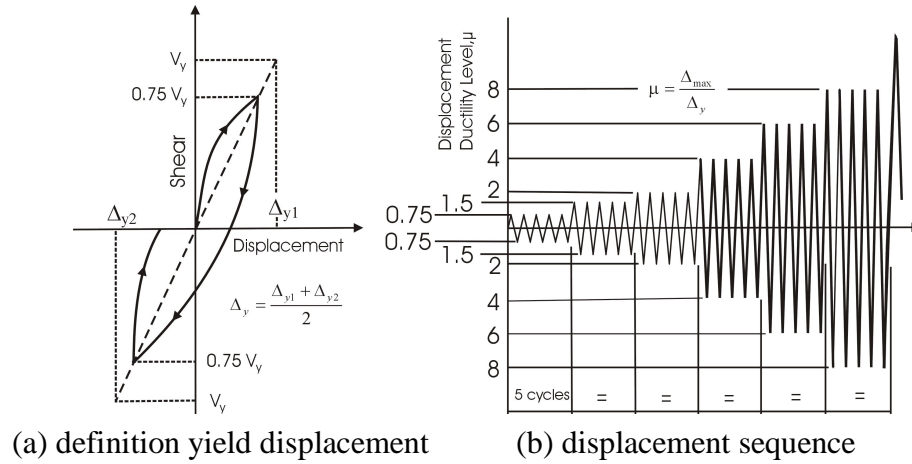


Figure 4: Sequence of imposed horizontal displacements (adapted from Ref. 4)

TEST RESULTS AND DISCUSSION

Behaviour of Columns Tested in Phase I

Figure 5 shows the normalized stress vs. strain curve of the confined concrete for phase I columns. The multiple load cycles applied to columns C05 and C07, as described previously, are not shown in the figure for clarity of the other curves. In addition, column C07 was loaded twice; in the first loading, the specimen could not be failed and then it was moved to a higher capacity testing machine for complete failure. Assuming full composite action between the longitudinal rebars and the concrete, the load carried by the concrete was obtained by subtracting the load carried by the longitudinal rebars (derived from the strain data) from the total column load. The concrete load vs. strain curves for all the columns are then converted to confined concrete stress, f_{cc} , vs. strain curves by dividing their ordinate by A_c (where, $A_c = A_g - A_{st}$). These curves are commonly referred to as confined concrete material curves. In order to compare directly the effect of confinement on the behaviour of the concrete in the columns, it is necessary to normalize the concrete material curves of the columns with respect to their unconfined concrete strengths, f'_{co} , taken as $0.85 f'_c$. These normalized curves are shown in Figure 5. It should be noted that the descending branches of these curves may not be accurate because of the localization of axial strains and lateral bending of the longitudinal bars in the test regions.

As expected, column C00A showed brittle failure because of the relatively wide spacing of the ties. The peak load for this column was achieved at a strain of 0.0035. Column C00B showed ductile failure because of the closely spaced hoops in the test region. The peak load was reached at an average strain in the test region of 0.0305, which is about nine times the analogous strain for column C00A. The enhancement in concrete strength due to confinement of 96% was obtained (based on concrete area enclosed by the centreline of the ties). Columns C01, C02, C03, and C04 with bolted collars, showed

ductile failure, although the ductility of column C04 was somewhat lower due to the relatively large collar spacing. The curve for column C05 is terminated just before cycling the load. From these curves it can be calculated that the average enhancement in concrete strength for columns with bolted collars (based on concrete area $A_c = A_g - A_{st}$) is 67% with a maximum value of 115% for column C05. The average strain at peak stress of confined concrete for these columns is 0.0285 with a maximum value of 0.045 for column C05 (after cycling the load). Columns C06, C07, C08, and C09, with welded collars, also showed enhancement in concrete strength and ductility. The average enhancement in concrete strength of 110% (based on the concrete core area, which for collared columns is A_c) was obtained for these columns with a maximum value of 131% for column C07. The average strain at peak stress of confined concrete for these columns was 0.0288 with a maximum value of 0.0350 for column C06. Although large strains at peak stress of confined concrete were observed for these columns, the failure exhibited was brittle due to the fracture of a corner weld in one or more of the collars. Nevertheless, improved column ductility would certainly have been exhibited had the collar welds not failed. It is also clear from the curves of Figure 5 that with an increase in collar spacing, the strength enhancement factor and the ductility of the column both decrease. This can be observed for bolted collars by comparing the results of columns C02, C04, and C05 and for welded collars by comparing columns C07 and C09. The flexural and axial stiffnesses of the collars (size of the collars) also have an effect on the behaviour of the columns. The increase in the stiffness of the collars increases both the strength and the ductility of the column. This can be observed for bolted collars by comparing the curves of columns C01 and C02 and for welded collars by comparing curves of columns C06, C07, and C08.

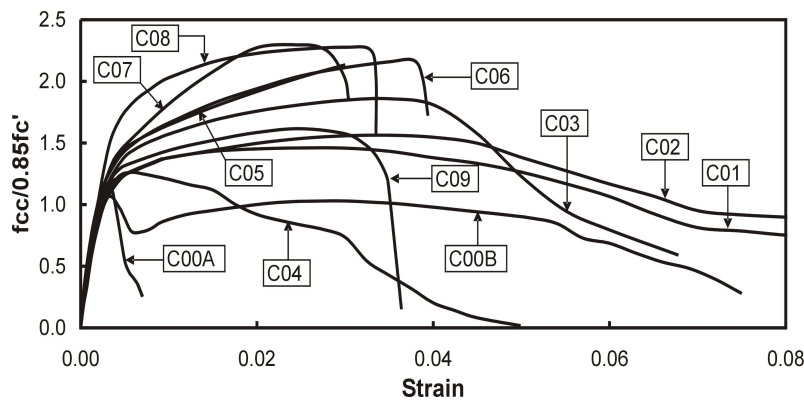


Figure 5: Normalized concrete confined material curves

A typical deformed bolted collar and fractured welded collar at the end of the tests are shown in Figures 2(f) and 2(g). The plastic flexural deformations are evident in the bolted collar. The appearance of three columns (C02, C04, and C05) at the end of the tests (with collars removed) that had different collar spacings but were otherwise identical are shown in Figures 2(c), 2(d), and 2(e). It is obvious from this Figure that no spalling of concrete took place under the collars. The localized damage seen in column C04 is a result of the relatively large collar spacing that resulted in less efficient confinement.

Behaviour of Columns Tested in Phase II

The axial loads and axial load indices for phase II columns are given in Table 2. It is to be noted that the stroke limit of the jack for horizontal loading was about 200 mm in either direction. The yield displacements and the number of complete cycles that were applied to these columns are given in Table 4.

The yield displacement corresponds to the point of application of horizontal load. The first five cycles for each column were performed using load control and the remaining cycles were performed using displacement control at the specified displacement ductility level. In specimens CL0, CL1, CL2, CL3, and CL4, the last ductility level at which cycles were performed corresponds to the displacement equal to the stroke of the jack (i.e., the starred number of cycles in Table 4), giving ductility levels of about 6.6, 8.6, 4.8, 5.2, and 7.1, respectively. The displacement ductility, μ_{Δ} , shown in Table 4 is different for columns CL1 and CL4 because they were failed monotonically as described subsequently. Columns CL1 and CL5 were tested under zero gravity load and columns CL2, CL3, CL4, CL6, CL7, and CL8 were tested under gravity load of 720 kN. The testing of column CL0 was started with a gravity load of 1470 kN, which was maintained up to the end of 16th cycle and then reduced to 720 kN.

Table 4—Yield displacement, total energy dissipated, μ_{Δ} , and number of cycles sustained

Specimens	Δ_y mm	Total Energy Dissipated KN·m	μ_{Δ}	Number of Complete Cycles Sustained								
				$V = 0.75V_y$	Displacement Ductility, μ_{Δ}							Total
					1.5	2	4	6	8	10	12	
CL0	30	1060	6.6	5	5	5	5	5	19*	-	-	44
CL1	23	732	12.9	5	5	5	5	5	20*	-	-	45
CL2	41	482	4.8	5	5	5	5	7*	-	-	-	27
CL3	38	1082	5.2	5	5	5	5	25*	-	-	-	45
CL4	28	977	10.9	5	5	5	5	5	20*	-	-	45
CL5	8	467	8.4	5	5	5	5	5	5	5	2	37
CL6	8.5	451	7.3	5	5	5	5	5	5	1	-	31
CL7	11.5	783	9.0	5	5	5	5	5	5	5	-	35
CL8	11	738	9.7	5	5	5	5	5	5	5	-	35

The upper limit for the number of complete cycles was 45. In order to facilitate this discussion, the first collar above the footing has been numbered as one, and the next collar as two, and so on. Specimens CL1, CL3, and CL4, all with long shear-span, did not fail at the completion of 45 cycles. The stroke of the jack was adjusted for these columns and then the columns were pushed in one direction (north) up to the available stroke limit of the adjusted jack, but these columns could not be failed. The column CL0 failed in shear in the 45th cycle at the location of hinge formation while pushing the column towards the north as depicted in Figure 6, accompanied by a reduction in both horizontal and vertical loads. An upward shift in the location of hinge formation has been observed for this column during the regime of cycling. Columns CL2, CL5, CL6, CL7, and CL8 failed due to fracture of the vertical bars under low cycle fatigue. In column CL2, the vertical bars became visible in the 22th cycle due to spalling of the concrete cover. The three vertical bars on the south face of the column fractured while pushing the column towards the north; one in each of 26th, 27th, and 28th cycle. The test was stopped after the fracture of the third vertical bar in the 28th cycle. In column CL5, the fracture of the two vertical bars took place on the south face of the column while pushing the column towards the north; one in each of the 37th and 38th cycle. The test was stopped in the 38th cycle after the rupture of the second bar. In column CL6, the test was stopped after the fracture of a single vertical bar (the middle bar) on the north face of the column while pushing the column towards the south in the 32nd cycle, accompanied by a drop in load. In column CL7, the test was stopped after the fracture of three vertical bars on the north and south faces of the column. The first vertical bar fractured on the south face while pushing the column towards the north in the 35th cycle, the second

vertical bar fractured on the north face while pushing the column towards the south in the 35th cycle. The third vertical bar also fractured on the north face while pushing the column towards the south in the 36th cycle and then the test was stopped. In column CL8, the middle bar on the south face fractured while pushing the column towards the north in the 36th cycle. While pushing the column towards the south in 36th cycle, two more bars fractured on the north face of the column, one after the other and the test was stopped.

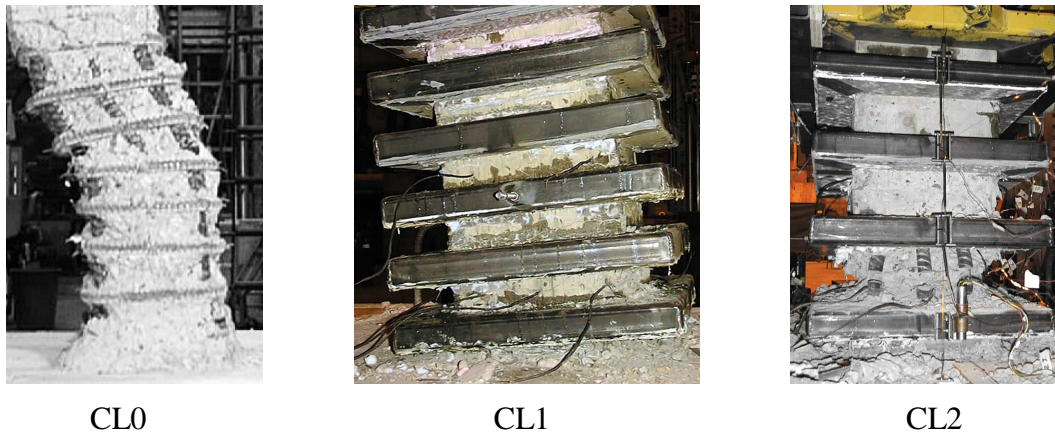


Figure 6: Appearance of typical phase II columns at the end of the tests

In column CL2, most of the damage occurred in the first two gaps—the gap between the first collar and the footing and the gap between the first and second collars—however, fracture of the vertical bars occurred in the second gap as depicted in Figure 6. In columns CL1, CL5, CL6, CL7, and CL8, most of the damage was concentrated in the gap between the first collar and the footing. The appearance of one of these columns at the end of the test, i.e., CL1, is also shown in Figure 6. A similar type of failure has also been observed by Xiao and Wu [5], who tested under cyclic loading thinly jacketed columns with stiffeners that resemble the HSS collars. The fracture of vertical bars of columns CL5, CL6, CL7, and CL8 also took place in the first gap. In column CL3 the damage was well distributed up to the fourth collar, and in column CL4, the damage was concentrated in the gap between the first and the second collar. The appearance of columns CL0, CL1, and CL2 at the end of the test in Figure 6, can also be considered typical of columns with closely spaced ties, closely spaced collars, and widely spaced collars, respectively. In the collared columns, very little spalling of concrete between the collars was observed at the end of the first 20 cycles, a ductility level equal to 4, which is commonly used for the design of new reinforced concrete structures in seismic zones. In the case of the conventional column (CL0), most of the spalling of the concrete cover occurred at a displacement ductility level of 1.5. Hence, collared columns possess a larger effective core than that of conventionally tied columns and are more resistant to degradation under severe cyclic loading. In addition, no slippage of collars was observed during cyclic loading; a feature which is highly desirable for the success of this rehabilitation scheme. In the collared columns, most of the spalling was confined to the lower half of the test region, while in the conventional column, spalling took place over a wider range (Figure 6).

Figure 7 shows the moment vs. lateral drift hysteresis curves of all the columns tested in phase II of the project. Generally, the hysteresis curves for columns under cyclic loading are represented in terms of horizontal load vs. lateral displacement at the point of application of the horizontal load. In the present study, the points of application of horizontal and vertical loads are at considerably different heights, especially in columns with short shear spans, hence, both horizontal and vertical loads contribute considerably to the applied moment at the critical section of the columns. Therefore, moment vs. lateral

drift relationships are considered to be more appropriate for presenting the hysteresis loops of columns tested in this phase.

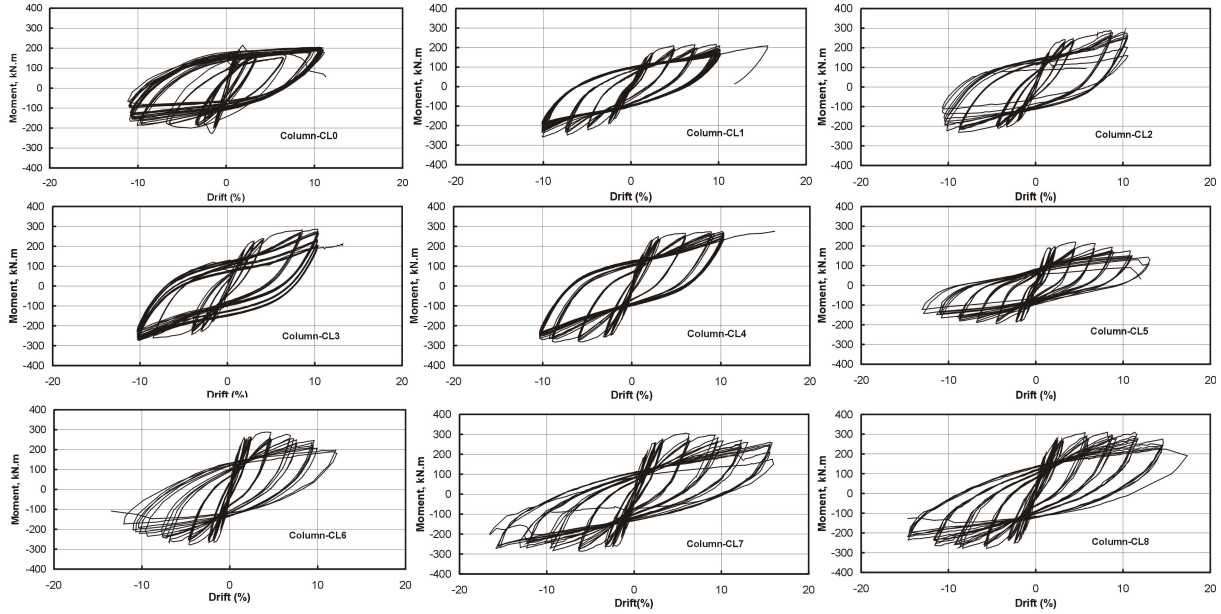


Figure 7: Moment vs. lateral drift hysteresis for all columns

There are several ways to express the ductility of the yielding structures. Among them, the most commonly used methods of measuring ductility of structural members are: (1) curvature ductility factor, μ_{ϕ} ; (2) rotational ductility factor, μ_{θ} ; and (3) displacement ductility factor, μ_{Δ} . Curvature ductility, μ_{ϕ} , represents the sectional behaviour of the member and local ductility in the hinging zone. The displacement and rotational ductility factors are used to express the overall behaviour of the members. These ductility factors are related to each other. In the columns under study, the moment distributions along the heights of the columns are complex due to the $P-\Delta$ effect; therefore, the relationships between the various ductility factors will also be complex, which is an area currently being studied. In the present paper, the displacement ductility factor, μ_{Δ} , will be presented for all the phase II columns. The displacement ductility factor is defined as:

$$\mu_{\Delta} = \frac{\Delta_u}{\Delta_y} \quad [1]$$

Where Δ_y and Δ_u are the yield displacement and ultimate displacement. The yield displacements are given in Table 4. The ultimate lateral displacement, Δ_u , can be found from the envelope curves to the moment vs. lateral drift hysteresis loops given in Figure 7. The ultimate horizontal drift corresponds to the moment equal to the 90% of the maximum moment in the descending branch of the envelope curves to the moment vs. lateral drift hysteresis loops. The displacement ductility factors thus calculated are given in Table 4.

For columns CL0 to CL4, there was no drop in the moment capacity up to the imposed displacement limited by the stroke of the jack. For columns CL0 and CL2, the maximum displacement—taken as the average of the two directions—exhibited by these curves was used as the ultimate displacement. For columns CL1 and CL4, the maximum displacement related to the final push in the north direction was taken as the ultimate displacement. For column CL3, the displacement related to the final push was not used because of the substantial reduction in the moment capacity due to degradation. For columns CL5 to CL8, the moment capacity declined with an increase in the drift at large displacements. Therefore, the drift corresponding to the moment in the descending branch equal to the 90% of the maximum moment capacity was taken as the ultimate drift.

The effect of shear span on the displacement ductility of the columns can be studied by comparing the ductility of columns CL1 to CL5 and CL4 to CL8. The displacement ductility of CL1 is higher than that of CL5 and the displacement ductility of CL4 is higher than that of CL8. The displacement ductility of CL2 cannot be compared to that of CL6 for this purpose because the lower displacement ductility of column CL2 may be attributed to the limit on the stroke of jack. Column CL3 was excluded from this comparison because of the degradation in moment capacity due to application of an excessive number of cycles before applying the final push towards the north. The increase in collar spacing has a detrimental effect on the displacement ductility and energy dissipation of the columns. This can be verified by comparing the displacement ductility and energy dissipation of columns CL2 to CL3 and CL6 to CL7. The axial load has a significant effect on the behaviour of the columns. It has an effect on the strain level of the column directly and through the P- Δ effect. Comparing the displacement ductility and energy dissipation of CL1 to CL3 it can be concluded that with the increase of axial load, the energy dissipation of the column increases and displacement ductility decreases.

The total energy dissipated by all the columns tested in phase II is given in Table 4. The dissipated energy in a cycle was determined by calculating the area enclosed by the moment vs. lateral drift hysteresis loops. The total energy dissipated by a column was determined by summing the energy dissipated in each cycle of loading. Figure 8a shows the energy dissipated in each cycle of a typical column (column C05). This column was subjected to 37 complete cycles before failure. At each ductility level five cycles were performed. The energy dissipated in the first cycle was generally higher than that of the other four cycles at the same ductility level. Figure 8b shows the cumulative energy dissipated by the column with respect to the number of cycles. The cumulative energy dissipated increases at an increasing rate with the increase of the displacement ductility level until the displacements become relatively large. This figure also shows that the cumulative energy dissipated by the column in the elastic range is negligible as compared to the energy dissipated by the column in the plastic range.

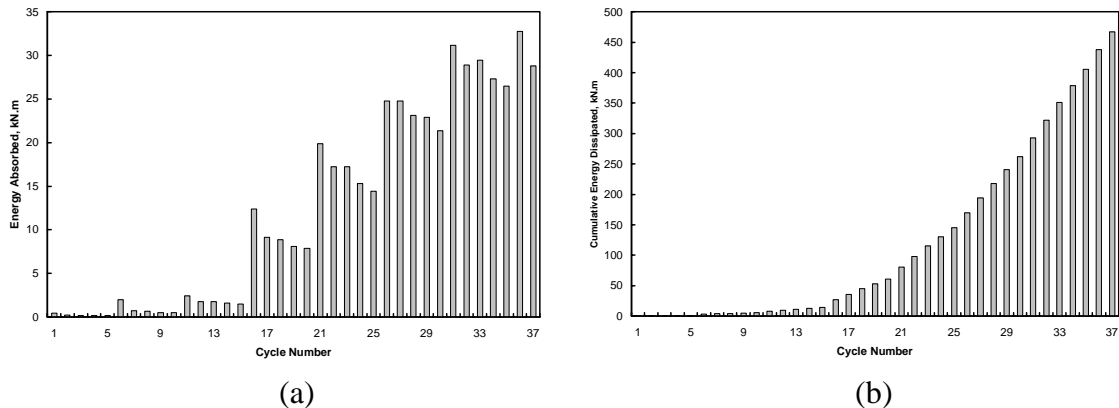


Figure 8: Energy dissipated by column C05: (a) per cycle; (b) cumulative

CONCLUSIONS

The behaviour of columns under concentric monotonic loading and under simulated seismic loading has confirmed that the external collar confinement can be used as a means of rehabilitation for seismically deficient reinforced concrete structures through enhancement in strength and ductility. The pertinent conclusions based on the test results of the first two phases of the project are presented below.

Based on the test results of phase I of the project it can be concluded that the collared columns exhibited a maximum strength enhancement of concrete of 131% (column C07), and a maximum observed strain at peak stress of 0.045 (column C05). By comparison, a conventionally confined column satisfying the plastic hinge requirements of ACI 318 and CSA Standard A23.3 (column C00B) exhibited a strength enhancement of concrete of 96%, calculated based on the core of the column, and a strain at peak stress of 0.030. The external confinement by HSS collars prevents the spalling of concrete cover under the collars and inhibits spalling between the collars. The effective core area of externally confined columns is therefore significantly larger than that of conventional columns and can be taken as the full cross-sectional concrete area.. On average, columns confined by collars having welded corner connections show an enhancement in strength of 2.41 times that of columns with bolted collars. The strain at peak stress of the concrete confined by the two types of collars are comparable and generally are close to ten times that which would be expected for unconfined concrete. The lower failure strain exhibited by columns with welded collars is attributed to the lack of ductility of the welds in the collars themselves and it may be increased significantly with deeper weld penetration.

Based on the test results of phase II of the project it can be concluded that collared columns showed very good seismic behaviour under severe cyclic loading. Reduction in the shear span has a detrimental effect on the ductility of the columns. With an increase in axial load on the column, ductility reduces and energy dissipation increases. With an increase of collar spacing, both energy dissipation and ductility reduces. In addition, no slippage of collars was observed and no spalling of concrete occurred under the collars during severe cyclic loading, a feature which is highly desirable for the success of this rehabilitation scheme. The desired enhancement in strength and ductility was achieved through confinement of the concrete and the presence of the collars made the columns very resistant to degradation under severe cyclic loading. External confinement by HSS collars is therefore an effective means of rehabilitating columns in seismically deficient reinforced concrete buildings.

ACKNOWLEDGEMENTS

This ongoing research program is funded by the Natural Sciences and Engineering Research Council of Canada. The high capacity universal testing machine in which two columns discussed in this paper were tested was provided by the Centre for Engineering Research in Edmonton, Canada. The authors are also grateful to Reliable Tubes Ltd., Unicon Concrete Ltd., and Master Builders for their donations in carrying out this project.

NOTATION

A_c	=	$A_g - A_{st}$; area of the concrete in the gross column cross-section, mm^2 ;
A_g	=	gross area of the section, mm^2 ;
A_{st}	=	cross-sectional area of longitudinal steel, mm^2 ;
A_t	=	cross-sectional area of one leg of the confining steel, mm^2 ;

E_s	=	modulus of elasticity of steel, <i>MPa</i> ;
f'_c	=	cylinder strength of concrete, <i>MPa</i> ;
f_{cc}	=	applied stress on confined concrete in column, <i>MPa</i> ;
f'_{co}	=	$0.85f'_c$; unconfined concrete strength of the column, <i>MPa</i> ;
f_y	=	yield strength of steel, <i>MPa</i> ;
f_p	=	peak stress of steel, <i>MPa</i> ;
H'	=	strain hardening modulus, <i>MPa</i> ;
s	=	center-to-center spacing of ties or collars, <i>mm</i> ;
s'	=	clear spacing between collars or ties, <i>mm</i> ;
Δ_u	=	ultimate horizontal displacement at the point of application of horizontal load, <i>mm</i> ;
Δ_y	=	horizontal displacement at the point of application of horizontal load at which yielding takes place, <i>mm</i> ;
ε_p	=	strain at peak stress of steel, f_p ;
ε_{sh}	=	strain at the start of strain hardening;
μ_ϕ	=	curvature ductility factor;
μ_θ	=	rotational ductility factor;
μ_Δ	=	displacement ductility factor;
σ	=	standard deviation of the concrete cylinder strength, <i>MPa</i> ;

REFERENCES

1. Driver, R.G., Kulak, G.L., Kennedy, D.J.L. and Elwi, A.E., "Cyclic test of four-story steel plate shear wall". *Journal of Structural Engineering*, ASCE, 1998; 124(2): 121-130.
2. Hussain, M.A. and Driver, R.G., "Finite element study on the strength and the ductility of externally confined rectangular and square concrete columns," *Proc., Canadian Society for Civil Engineering Annual Conference*, Victoria, BC, Canada, May 30-June 2, 2001.
3. Hussain, M.A., Sharif, A., Basunbul, I.A., Baluch, M.H., Al-Sulaimani, G.J. "Flexural behavior of precracked reinforced concrete beams strengthened externally by steel plates". *ACI Structural Journal*, 1995; 92(1): 14-22.
4. Ghee, A.B., Priestley, M.J.N. and Paulay T., "Seismic Shear Strength of Circular Reinforced Concrete Columns". *ACI Structural Journal*, January-February 1989: 45-59.
5. Xiao, Y., and Wu, H., "Retrofit of reinforced concrete columns using partially stiffened steel jackets," *Journal of Structural Engineering*, ASCE, May-June 2003; 129(6): 725-732.